



Contribution of Sentinel 1 Radar Data to Flood Mapping in the San-Pédro River Basin (South-west Côte d'Ivoire)

**Kouakou Hervé Kouassi^{1*}, Yao Alexis N'go², Anoh Kouao Armand¹,
Tanoh Jean-Jacque Koua¹ and Cristian Constantin Stoleriu³**

¹*Environmental Sciences and Technologies Laboratory, Jean Lorougnon Guédé University, P.O. Box 150, Daloa, Côte d'Ivoire.*

²*Laboratory of Geosciences and Environment, UFR Environmental Science and Management, Nangui Abrogoua University, Abidjan, Côte d'Ivoire.*

³*Department of Geography, Faculty of Geography and Geology, Alexandru Ioan Cuza University, Romania.*

Authors' contributions

This work was carried out in collaboration among all authors. Author KKH designed the study, treat the remote sensing data and wrote the first draft of the manuscript. Author NYA designed also this study and helped in the data acquisition. Authors AKA and KTJJ seconded the author KKH. Author SCC supervised the works. All authors read and approved the final manuscript.

Article Information

DOI: 10.9734/AJGR/2020/V3i230101

Editor(s):

(1) Xu Chong, Institute of Geology, China.

(2) Hani Rezgallah Al-Hamed Al-Amoush, Al al-Bayt University, Jordan.

Reviewers:

(1) Oluwole Ayinde Oyedeji, Pan African University, Nigeria.

(2) Jianhui Yang, Henan Polytechnic University, China.

Complete Peer review History: <http://www.sdiarticle4.com/review-history/55959>

Received 28 January 2020

Accepted 03 April 2020

Published 08 April 2020

Original Research Article

ABSTRACT

Floods result from the overflow of water which submerges the surrounding land. They are frequent on the coast of Côte d'Ivoire during the rainy season and have more or less serious consequences on the populations, property and the environment. The study site is the San Pedro river basin. It is a coastal catchment area characterized by an average annual rainfall of up to 2000 mm and subject to recurrent flooding. The objective of this study is to assess the risk of flooding during the great rainy season of 2017. The study aims to study flood hazard, assess vulnerability and map flood risk areas. The methodological approach is based on the use of C-band (5.6 cm) radar remote sensing

*Corresponding author: E-mail: kh.kouassi@gmail.com;

data acquired by the Sentinel-1 sensor at 12-day intervals. These data are in GRD (Ground Range Detected) level 1 format and were used to calculate the radar backscatter coefficient. The results obtained allowed to map the extent of the flooded areas and showed that more than 6,000 ha of land is flooded for more than 3 days. Sentinel-1 has enormous potential to identify flooding risky areas and to continuously monitor them.

Keywords: Floods; Radar remote sensing; Sentinel-1; San Pedro.

1. INTRODUCTION

Floods are submergence of land by water. Floods cause quite critical situations [1]. Floods are regular on the coast of Côte d'Ivoire, where the rainfall is abundant. The city of San Pedro has many socio-economic interests, namely: port, industrial, residential and agricultural areas. However, the recent floods observed in this city weaken these interests. Indeed, these floods cause considerable damage every year, destroying bridges, roads, habitats, plantations and bereaving several families.

The mapping of flood risk areas is a prerequisite and fundamental condition for any development and flood risk management program in the San Pedro River catchment area. Indeed, this mapping helps to choose development according to the diversity of the stakes present along a river and facilitates land use planning by better taking into account the risk of flooding [2].

Several studies are carried out for the mapping of the flood risk in San Pedro. So far, none of them has been carried out at the scale of the San Pedro river basin. Hence the need for this study entitled: Contribution of Sentinel-1 images for the mapping of flood risk areas in the San Pedro river basin (South-West of Côte d'Ivoire). The main purpose of this article is to study the floods during the great rainy season of 2017.

Several authors Cazals et al. [3], Romanescu et al. [4], Psomiadis et al. [5], Devranche et al. [6] use remote sensing data to map the extent of floods. The study of flooding is not difficult with optical remote sensing data because the period of the study (June and July) is particularly cloudy. The acquisition of radar data is independent of weather conditions. The study was carried out using C-band (5.6 cm) radar data acquired by the Sentinel-1 sensor at 12-day intervals. These data have a greater ability to penetrate the natural environment. Several authors, including Cazals et al. [3] and Clement et al. [7] have used these data for flood mapping.

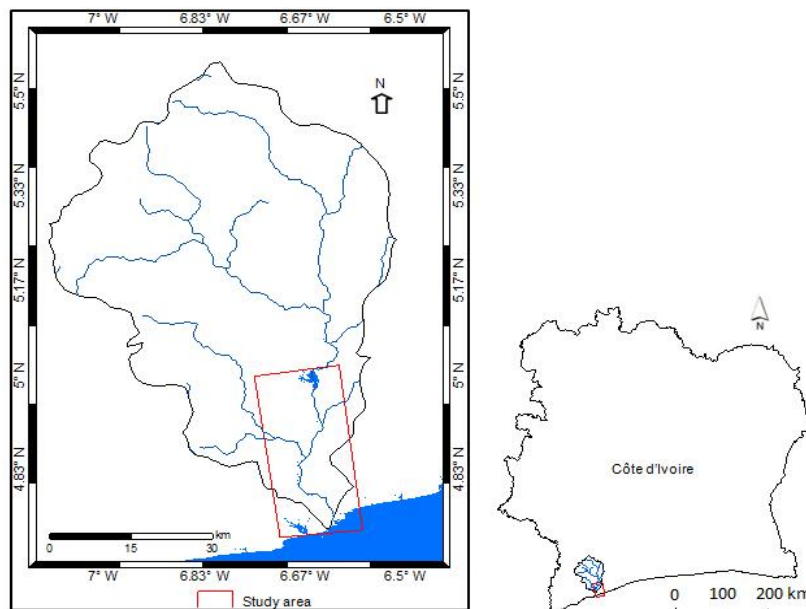


Fig. 1. Study area

1.1 Study Area

The study area is the San Pedro River basin. This coastal catchment area is located in the southwest of Côte d'Ivoire, between latitudes 6° 29" and 6°42" north and longitudes between 4° 51" and 9°32" west. It has many socio-economic interests, namely: port and industrial areas, residential areas, Taï National Park, etc. It is bordered by the department of Soubré in the north, the Atlantic Ocean in the south, the department of Sassandra at the east and by the Tabou department at the west.

The climate is characterized by two rainy seasons (a long season from April to mid-July

and a short one from September to November) and two dry seasons (a short one from mid-July to August and a large one from December to March). The flood period coincides with the long rainy season. The rains are abundant and can reach 2,000 mm per year (Fig. 2).

Hydrography is characterized by the San Pedro River and its tributaries (Fig. 1). The San Pedro river basin is a coastal watershed. A hydroelectric dam, Fayé Dam, is built on the river, 25 km north of the town of San Pedro.

The watershed is characterized by frequent flooding (Fig. 3). They cause considerable

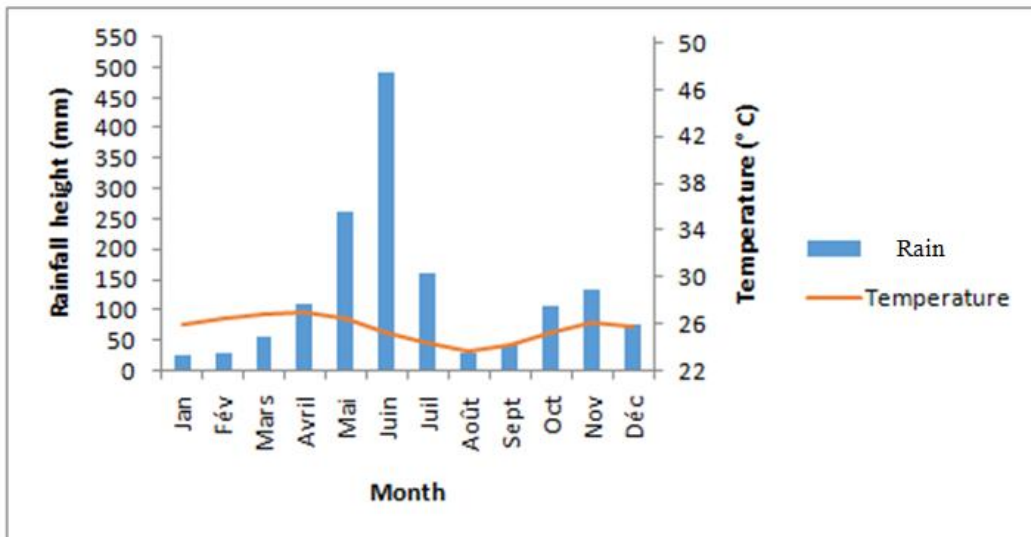


Fig. 2. Ombrothermal diagram of San-Pedro 2018



Fig. 3. San-Pédro flood
(Source: AIP)

damage each year, including the destruction of bridges, roads, habitats, crops and loss of human life. It results in population displacement and financial damage.

2. MATERIALS AND METHODS

2.1 Materials

The radar data used is recorded by the Sentinel-1 satellite. These are GRDH (Ground Range Detected High), VV / VH and C ($\lambda = 5.6$ cm) polarized and ascending images. The data cover the period from May to July corresponding to the flood period. Several Sentinel-1 (ascending orbit) images were used, including 5 during the major rainy season (June 16, 2017, June 28, 2017 and July 10, 2017) and the other non-floodable images (February 21, 2017).

These data are freely distributed by ESA and are available on the following website: <https://scihub.copernicus.eu/> (Table 1). The SNAP (Sentinel Application Platform) software developed by ESA has been used for the various processing operations. SNAP is available on the following website: <https://step.esa.int/main/download/>

The rainfall data for June and July 2017 on the catchment area of the San-Pédro River were used in this study. These data are provided by SODEXAM (Société d'Exploitation Aéroportuaire et Météorologique).

2.2 Methods

2.2.1 Pre-processing of the radar images

The pre-processing of the radar images (Sentinel-1) consisted of performing all the necessary operations before the main analysis and extraction of information. This involves performing radiometric calibration of the radar images, multi looking, correcting the geometric distortions and reducing the speckle.

To facilitate image comparison and multi-temporal analyses, it is essential to normalize the intensity of the backscattered signal. This normalization is carried out by radiometric calibration of the images. This consisted of calculating the backscattering coefficient as follows [8]:

$$\sigma^{\circ} (dB) = 10 * \log_{10}(\sigma^{\circ}) \quad (1)$$

With

$$\sigma^0(\theta) = \frac{DN^2 \sin \theta}{K} \quad (2)$$

DN is the numerical value of each pixel (Digital Number),

K is the calibration constant, it depends on the incidence angle and the polarization mode.

Multilooking allowed to have square pixels on the ground and to reduce the speckle. To perform multi looking, it is necessary to find the average pixel size along with the P_{range} radar sight and to project it on the ground using the incidence angle at the center of the scene θ_c according to equation 3. P_{range}^{ground} is the size of the pixel on the ground.

$$P_{range}^{ground} = \frac{P_{range}}{\sin(\theta_c)} \quad (3)$$

We then calculate the following ratio to know lines number to average. P_{az} is the pixel size in azimuth.

$$\frac{P_{range}^{ground}}{P_{az}} \quad (4)$$

The use of SAR radar images simultaneously with other sources of information (optical images, GPS) requires that they be correctly georeferenced. Thus, all the images used were georeferenced in the WGS 84 geodetic system and in the UTM projection in zone 29 North. After this, the filter used to remove the speckle is proposed by Lee et al. [9].

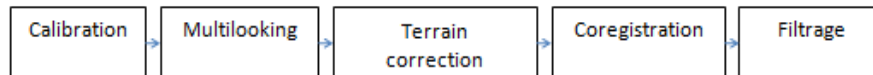
2.2.2 Detection of flooded areas

Flooded areas have lower backscatter on radar images due to specular reflection when the signal interacts with a smooth surface such as water surfaces. It has been possible to isolate flood zones by simply calibrating the numerical values of the radar backscatter coefficient. Indeed, the thresholding of an image makes it possible in particular to identify and isolate certain values identifying objects having the same spectral characteristics (Fig. 4). Several authors, including Maniruzzaman et al. [10] Cazals et al. [3] use this method. Pixels in flood zones have values below -15 dB. All pixels whose numerical value is below the threshold value of -15 dB are assigned to the class "flooded areas".

Table 1. Sentinel-1 radar data characteristics

Polarization	VV/VH
Band	C ($\lambda=5,6$ cm)
Spatial resolution	20 x 22 m ² (az. x gr. range)
Pixel size	10 x 10 m ² (az. x gr. range)
Swath width	250 km
Incidence angle	36°-42°
Equivalent Number of Looks	4.9
Format	GRDH
Dates	2017: 4, 16, 28 June ; 10 July

Source: <https://scihub.copernicus.eu/>



Scheme 1. Flow chart showing processing of radar images

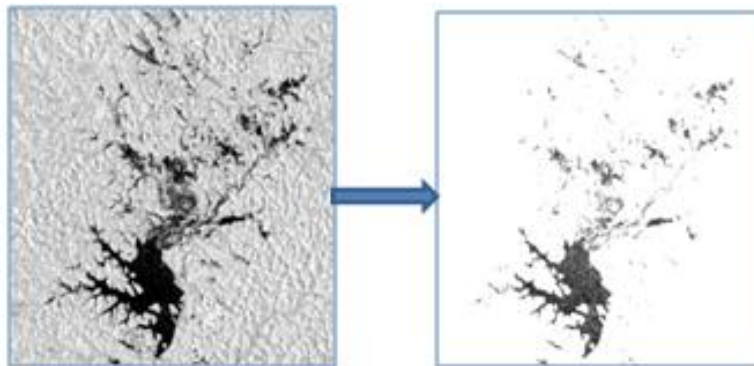


Fig. 4. Detection of flooded areas

3. RESULTS AND DISCUSSION

3.1 Flood Mapping

Sentinel 1 data allow a better distinction of floods and highlight the magnitude of the floods. Indeed, floods extend over a large area (Fig. 5). The images acquired before and after the floods provide immediate information on the extent of the floods and allow the assessment of material and environmental damage. The flooded areas were delineated with high precision.

The flooded areas vary according to the rainy periods, however, their areas all remain significant in the San Pedro River catchment (Fig. 6). The flooded areas are located around the shallows.

The areas of flooded zones are 6,007 ha for June 10, 2017. The results show a regression of the flooded areas. The flood coverage area increased from 6,007 ha to 2,426 ha in 12 days. Then there is an increase of flooded areas which

extend from 2,426 ha on June 28, 2017, to 3,549 ha on July 10, 2017.

C-band (5.6 cm) radar data acquired by the Sentinel-1 sensor with 12 days intervals were used for flood mapping during the major rainy season in the San Pedro river basin. Indeed, one of the advantages of using satellite data to map the extent of floods is the possibility of identifying large-scale rainfall floods far from the flood plains [11]. Sentinel-1 data is generally available a few hours after the satellite has passed, allowing near-real-time analysis of the flooding stretching. The results also make it possible to estimate the flooded areas by using Sentinel 1 data. The present study allowed to map and estimate the flooded areas. The results confirm the works of several authors including Cazals et al. [3] and Psomiadis et al. [5]. Indeed, these authors also used Sentinel 1 radar data for mapping and spatiotemporal monitoring of floods. It appears that sentinel 1 radar data offers enormous potential for mapping and spatiotemporal monitoring of floods.

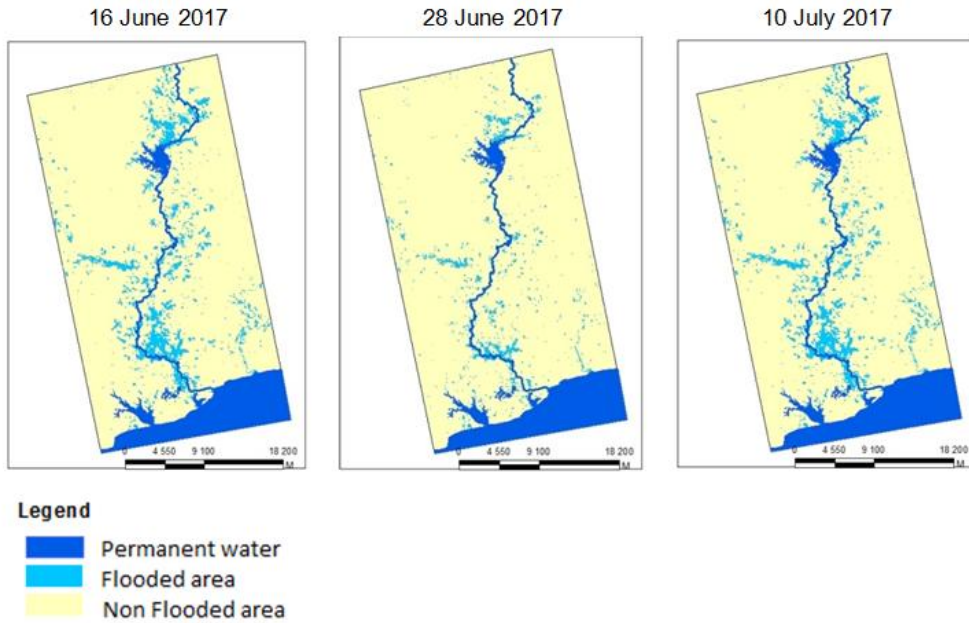


Fig. 5. Highlighting of flooded areas during June and July 2017

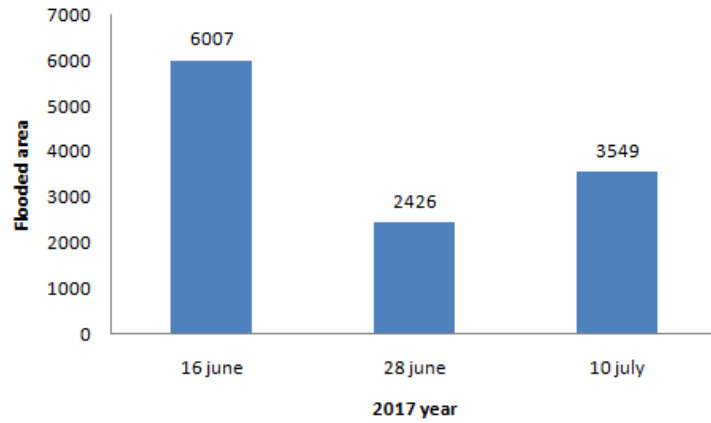


Fig. 6. Flooded areas in June and July 2017 in the San-Pedro river basin

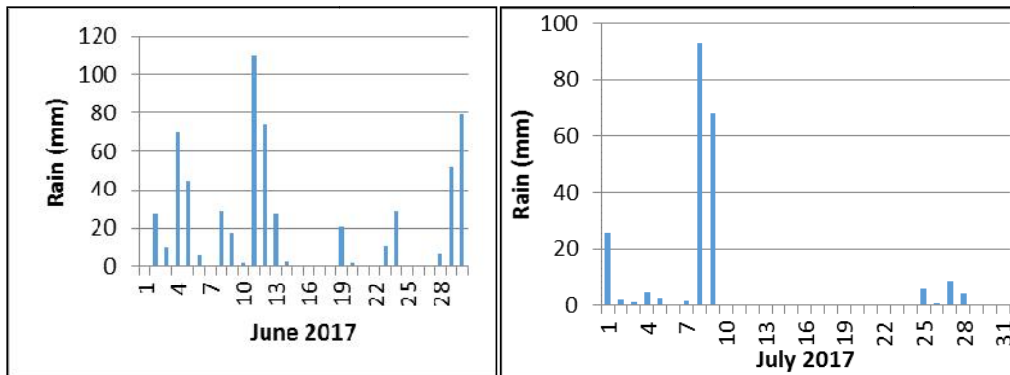


Fig. 7. Rainfall for June and July 2017 at the San-Pedro pumping station

3.2 Analysis of Rainfall Data

Fig. 7 shows the rainfall amounts in the San Pedro river basin during June and July 2017. During June, it rains practically every day, with rainfall heights exceeding the criticality threshold, which is of the order of 40 to 50 mm. The 11th June records a maximum height of 115 mm and the 8th July, 93 mm. These rainfalls in the San Pedro river basin are described as extreme rainfalls.

This study shows that extreme rains and long rains of moderate-intensity are largely responsible for the floods. This confirms the work of Saley [12] who worked in the west of Côte d'Ivoire. Their work shows that the floods in the humid tropical zones are mainly due to intense rains or medium and long duration rains.

Following the heavy rainfall during the week of June 12 to 30, the month of June 2017 is characterized by record rainfall in the San Pedro river basin. Nearly 178.6 mm fell on the San Pedro river basin. These large quantities of water brought by these rains in less than 24 hours quickly saturate the soil. The rapid saturation of the soil generates rushes that lead to flooding in the San-Pedro river basin. Radar data has allowed mapping the flooded areas.

4. CONCLUSION

The objective of this work is the knowledge improvement of the flood hazard at the scale of the San Pedro river basin. To meet this objective, a time series of 3 Sentinel-1 radar images with an interval of 12 days, of VV/HV polarizations, was analyzed. These images recorded the 16th, 28th June and 10th July 2017 were used for mapping of flooded areas. A thresholding method was used to isolate the numerical values of the radar backscatter coefficient corresponding to flooded areas. It distinguishes the classes the flooded areas (open water and flooded vegetation) and non-flooded areas. The results obtained allowed to map the extent of the flooded areas. The areas of the flooded areas are 6,007 ha for 10th June, 2017, 2,426 ha for 28th June, 2017, and 3,549 ha for the 10th July, 2017. Rain data show that the origin of the floods is due to the extreme rains that fell over the study areas in June and July 2017. Indeed, the rains reached 115 mm in 24 hours the 11th June.

The results obtained show that the contribution of Sentinel-1 data for flood mapping is significant.

The potential of Sentinel-1 data to monitor flooding would, therefore, be an asset. Furthermore, the information obtained during this study can contribute to the development of flood zones for more thoughtful urbanization. It can also help to identify wetlands suitable for certain activities.

COMPETING INTERESTS

Authors have declared that no competing interests exist.

REFERENCES

1. Mamadou I, Alassane OS, Malam AM, Garba Z. Risques d'inondation et proposition d'un plan d'évacuation des eaux de pluie dans la ville de Kantché, Région De Zinder Au Niger. *European Scientific Journal*. 2019;15(35):88-104.
2. Karrouchi M, Touhami MO, Oujidi M, Chourak M. Cartographie des zones à risque d'inondation dans la région Tanger-Tétouan: Cas du bassin versant de Martil (Nord du Maroc). *International Journal of Innovation and Applied Studies*. 2016;14(4): 1019-1035. French.
3. Cazals C, Rapinel S, Frison P-L, Bonis A, Mercier G, Mallet et al. Mapping and characterization of hydrological dynamics in a coastal marsh using high temporal resolution sentinel-1A images. *Remote Sensing*. 2016;8(7):570.
4. Romanescu G, Cimpianu CI, Miheu-Pintilie A, Stoleriu CC. Historic flood events in NE Romania (post-1990). *Journal of Maps*. 2017; 13(2):787–798.
5. Psomiadis E, Soulis KX, Zoka M, Dercas N. Synergistic approach of remote sensing and GIS Techniques for flash-flood monitoring and damage assessment in the Thessaly plain area, Greece. *Water*. 2019;11(3):448-469. Available: <https://doi.org/10.3390/w11030448>.
6. Devranche A, Poulin B, Lefebvre G. Mapping flooding regimes in Camargue wetlands using seasonal multispectral data. *Remote Sens. Environ.* 2013;138:165–171. Available: <https://doi.org/10.1016/j.rse.2013.07.015>
7. Clement MA, Kilsby CG, Moore P. Multi-temporal synthetic aperture radar flood mapping using change detection. *J Flood Risk Management*. 2018;11:152–168.

8. Rosenqvist A, Shimada M, Ito N, Watanabe M. Alos palsar: Apathfinder mission for global-scale monitoring of the environment. *IEEE Trans. Geosci. Remote Sensing.* 2007;45:3307–3316.
9. Lee JS, Jurkevich T, Dewaele P, Wambacq P, Oosterlinck A. Speckle filtering of Synthetic Aperture Radar images: A review. *Remote Sensing Reviews.* 1994;8:313–340.
10. Maniruzzaman Sk, Balaji S, Sharma SV. Sivaprasad. Flood inundation mapping using synthetic aperture radar (SAR) data and its impact on land use/land cover (LULC): A case study of Kerala flood 2018, India. 2020;13(3):46-53.
11. Anusha N, Bharathi B. Flood detection and flood mapping using multi-temporal synthetic aperture radar and optical data. *The Egyptian Journal of Remote Sensing and Space Science.* 2019; S1110982318303041. Available:<https://doi.org/10.1016/j.ejrs.2019.01.001>.
12. Saley MB, Kouamé FK, Penven MJ, Biémi J, Kouadio HB. Cartographie des zones à risque d'inondation dans la région semi-montagneuse à l'ouest de la Côte d'Ivoire: Apports des mna et de l'imagerie satellitaire. *Téledétection.* 2005;5(3):53-67.

© 2020 Kouassi et al.; This is an Open Access article distributed under the terms of the Creative Commons Attribution License (<http://creativecommons.org/licenses/by/4.0>), which permits unrestricted use, distribution, and reproduction in any medium, provided the original work is properly cited.

Peer-review history:

*The peer review history for this paper can be accessed here:
<http://www.sdiarticle4.com/review-history/55959>*